

NASA-CR-197192

NASw-4435

# A MAGNETIC SHIELD/ DUAL PURPOSE MISSION

N95-13006

Unclas

G3/18 0026180

FINAL REPORT: 1993-1994

NASA/USRA Advanced Design Program

by

(NASA-CR-197192) A MAGNETIC  
SHIELD/DUAL PURPOSE MISSION Final  
Report, 1993 - 1994 (Duke Univ.)  
26 p

Duke University  
Department of Mechanical Engineering and Materials Science  
Durham, North Carolina 27708-0300

July, 1994

Professor Franklin H. Cocks  
Seth Watkins

## ACKNOWLEDGMENTS

The assistance provided by Eric Smith and Rich Hines at the Vesic Engineering Library at Duke University is gratefully acknowledged. The enormously helpful input from our mentor, Don Carson, at Goddard Space Flight Center, is also gratefully acknowledged. The support of the USRA Advanced Design Program and the North Carolina Space Grant Consortium has been essential in this academic endeavor.

The following students have contributed to this design effort and to the writing of this report: Jamil Albertelli, R. Braden Copeland, Eric Correll, Chris Dales, Dana Davis, Nechole Davis, Rob Duck, Sandi Feaster, Patrick Grant, Mack Haynes, Douglas Jarrard, Andrew Konop, John Koon, Stu Levy, Dwight Lowie, Scott Miller, John Murnane, Howard Nelson, Matt Pangaro, Jack Perkins, Malcolm Peverley, Audra Plenys, Michael Reams, George Robbins, Christopher Salter, Bobby Santos, Glen Schumacher, Kara Slade, Jon Slagel, Mark Slominski, Marcus Smith, Terence Sobolewski, Tim Sovich, Hermes Soyez, Martin Stalheim, Matt Swecker, David Zavelson

## Table of Contents

Abstract.....	4
Overview.....	5
Payload Design.....	6
Cryostat Design.....	6
Coil Design.....	8
Coil Charging.....	10
Instruments.....	11
Telemetry.....	12
Power.....	13
Predicting Orbital Effects of the Ship's Field.....	13
Scientific Experiment.....	14
Coil Orientation.....	16
Mass Shielding for the Payload.....	17
Conclusion.....	19
Appendix A.....	22

## Abstract

The objective of this work is to design, build, and fly a dual-purpose payload whose function is to produce a large volume, low intensity magnetic field and to test the concept of using such a magnetic field to protect manned spacecraft against particle radiation. An additional mission objective is to study the effect of this moving field on upper atmosphere plasmas. Both mission objectives appear to be capable of being tested using the same superconducting coil. The potential benefits of this magnetic shield concept apply directly to both earth-orbital and interplanetary missions. This payload would be a first step in assessing the true potential of large volume magnetic fields in the U.S. space program. Either converted launch systems or piggyback payload opportunities may be appropriate for this mission.

The use of superconducting coils for magnetic shielding against solar flare radiation during manned interplanetary missions has long been contemplated and was considered in detail in the years preceding the Apollo mission. With the advent of new superconductors, it has now become realistic to reconsider this concept for a Mars mission. Even in near-earth orbits, large volume magnetic fields produced using conventional metallic superconductors allow novel plasma physics experiments to be contemplated. Both deployed field-coil and non-deployed field-coil shielding arrangements have been investigated, with the latter being most suitable for an initial test payload in a polar orbit.

## Overview

Solar flares produce a significant increase in energetic particle activity in space. Flares typically last from 1 to 100 minutes and release energy in the range of  $10^{29}$  to  $10^{31}$  ergs. A full cycle of solar flare activity may last for several days, during which time any humans exposed would receive fatal doses of radiation. Flares may actually accelerate protons to energies approaching 50 GeV.<sup>1</sup> For practical purposes it is more important to consider the full distribution, which for solar flare radiation has an intensity peak between 50 and 100 MeV. As the particles approach the Earth, many get trapped in a band of warm plasma at an altitude between 4 and 10 Earth radii. The particles remain in that band for a short period, during which they dissipate energy and disperse. Geostationary satellites are especially vulnerable to these conditions, since their orbits are typically at an altitude of 6.6 Earth radii.<sup>2</sup> While satellites in low Earth orbit are protected by the Earth's magnetosphere, satellites with orbits having a semi major axis of 42,000 km (i.e., geostationary)<sup>3</sup> are outside the natural protection afforded by the magnetosphere.

Beyond the magnetosphere but in the general vicinity of the Earth, the radiation environment includes solar wind, cosmic rays, energetic ions from the sun, as well as energetic electrons from both the Sun and Jupiter. Solar wind generally does not have a strong effect on satellites, but it does affect the fluctuations of the Earth's magnetic field. Thus, the solar wind can cause violent and unpredictable magnetic storms.<sup>4</sup> In the general vicinity of the Earth, cosmic radiation consists of 83% protons, 13% alpha particles, 1% nuclei with atomic mass greater than 2, and 3% electrons. This combination of particles has an energy range of a few hundred to  $10^{14}$  MeV. The critical factor of intensity is solar cycle dependent,<sup>5</sup> but the flux is approximately  $1/\text{cm}^2\text{-sec}$  and the dose rate is less than  $10^{-4}$  rad/hr.<sup>6</sup> Energetic particles are much more powerful; a flux of energetic protons of greater than or equal to 5 MeV from a large solar flare can reach  $10^5/\text{cm}^2\text{-sec-steradian}$ . The dose rate from such a flare would exceed 100 rads/hr.<sup>7</sup>

Solar flare radiation would be a major health hazard outside the protection of the magnetosphere. Current manned space missions are at sufficiently low orbits that there is little concern about radiation. Apollo missions, however, which were high enough to encounter this radiation, were run at periods of low solar activity to minimize radiation exposure.<sup>8</sup> Humans traveling on interplanetary missions could not expect to escape the periods of intense energetic particle release which pose life threatening conditions.

In addition to magnetic shielding from the Earth, the equivalent of  $1000 \text{ g/cm}^2$  of mass shielding is provided by the Earth's atmosphere.<sup>9</sup> Using a pure mass protection concept, a dense material shield of hundreds of  $\text{grams/cm}^2$  would be necessary to reduce cosmic ray doses to levels close to Earth surface background. This would also apply to a long-term deployed space station in low earth orbit. Due to the inherent weight restrictions and volume management, mass shielding is

clearly impractical for protection against cosmic and galactic proton radiation during interstellar travel.

### **Payload Design**

The intent of this design project is to develop a feasibility study of a magnetic shielding experiment using a low temperature superconducting coil. The coil will be stationary (i.e., not deployed), and will be used (1) to protect a given payload volume from incident charged particles, (2) to examine the effects of a magnetic field on radio interference, (3) to examine the microcirculatory effects of passing a large magnet through a terrestrial charged particle environment, and (4) to use the earth's magnetic field to generate a voltage when the superconducting coil goes normal.

The basic payload limitations include a maximum weight of 480 pounds, launch into a 100 km earth orbit, and coil superconductivity for sufficient time to achieve the aforementioned experimental objectives.

### **Cryostat Design**

The cryostat is an essential part of the overall design of the proposed experimental system. In order for the coil to operate at a superconducting state, the temperature of the coil must be maintained at 4.2 K. It is expected that superconductivity will be required for a minimum of 40 hours. The function of the liquid helium cryostat is simply to maintain that temperature for the operational lifetime of the superconducting coil, which would be launched in the persistent field mode. The main limitation for the proposed experiment will be the allowable mass, which imposes considerable design restrictions on cryostat size and concomitant helium capacity. The cryostat will be fabricated from Type 304 stainless steel, with internal insulating layers. The cryostat completely surrounds the coil, which is surrounded by the liquid helium. An outer layer of liquid nitrogen has been considered, but is unnecessary due to the short mission duration. More helium, rather than nitrogen, can thus be used. Additionally, the nitrogen is significantly heavier than the helium. The inner radius of the cryostat will be approximately 5 cm. The cryostat is expected to have a mass of approximately 70 kg. The overall cryostat design is shown in Figure 1, and the cross-section is shown in Figure 2. The mounting and securing hardware is especially important due to the tremendous stresses experienced during launch, as well as the vibrational effects. The use of several mounting plates with "feed-through" design has been chosen for mounting purposes, as shown in Appendix A.

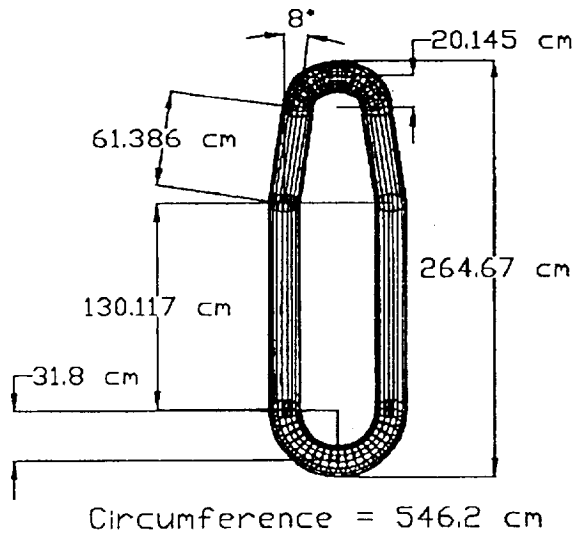


Figure 1 Overall Cryostat Design

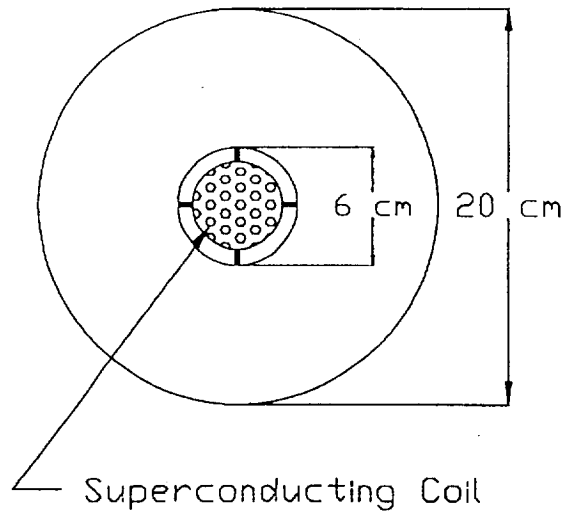


Figure 2 Cryostat Cross-section

## Coil Design

A number of assumptions have been made regarding the design parameters of the coil. Due to the poor mechanical and electrical properties of current high temperature superconductor wires, low temperature superconducting wire has been chosen for use in this experiment. Niobium titanium superconducting wire will be employed, which requires cooling to liquid helium temperature. Coil sizing requirements are such that the cross-sectional area ratio of copper sheathing to NbTi be 1.8 to 1, the overall wire diameter is 28 mils, the design current is 320 amperes per wire (as viewed through the cross section), and it is assumed that the wire will weigh 3.77 kg per kilometer. Conservatively, the wire critical current is estimated at 200,000 A/cm<sup>2</sup>. For design considerations, it is assumed that the coils will be packed in a hexagonal close packed bundle, with a packing factor of 0.74 (74% of the available space is utilized). One coil is required for the experiment. Due to potential magnetic flux interactions, it is anticipated that the best configuration for the coil design will be a twisted format, with the average twist density being 2 twists per inch. This ensures that eddy currents will not prevail in the coil, causing significant flux difficulty.

The intent of the experiment is to protect as much of the payload enclosure as possible from incident radiation, within the design constraints of weight and size. It should be noted that the effective Störmer radius is actually 40 percent of that calculated using the Störmer equation.

A computer code has been constructed to optimize the coil design based on known parameters. The mathematical basis for the design relies on the Störmer equation for protected dimension,  $C_{st}$ , known as the Störmer radius. This dimension measures the magnetically protected region, although as previously mentioned complete protection is only afforded to approximately 40% of that characteristic length. The dimension, measured in meters, is found as follows:

$$C_{st} = \sqrt{\frac{q\mu_o M}{4\pi P}} \quad (1)$$

where	q	=	the particle charge
		=	1.9 x 10 <sup>-19</sup> C
	μ <sub>o</sub>	=	the permeability of free space
		=	4π x 10 <sup>-7</sup> H/m
	P	=	the relativistic particle momentum (kg·m/s)
	M	=	the magnetic moment (ampere turns · m <sup>2</sup> )

Given a desired Störmer radius and momentum of particle to protect from, the magnetic moment can be found from equation 1.

In order to determine the required coil mass and the required cryostat mass, the number of turns per coil,  $n$ , is found using the following relation:

$$n = \frac{M}{iA} \quad (2)$$

where  $i$  = maximum current per wire  
 = 320 A (as specified above)  
 $A$  = the area enclosed by the loops forming the coil

The mass of the coil is thus found as follows:

$$m_{coil} = \Psi C n N \quad (3)$$

where  $\Psi$  = mass per unit length of NbTi wire  
 =  $3.77 \times 10^{-3}$  kg/m  
 $C$  = circumference of coil  
 $N$  = total number of coils

For the purposes of this design feasibility study, the total number of coils is assumed to be one. Then, for a given circumference, the mass of the coil can be determined. The cryostat mass is found in a similar manner:

$$m_{cryo} = \zeta C N \quad (4)$$

where  $\zeta$  = mass per unit length of the cryostat  
 = 3.4 kg/m

Finally, the total mass is that of the coils and cryostat.

The cross-sectional area of each coil must be found in order to ensure that the coil can be contained within specified cryostat dimensions. The total cross-sectional area of each coil can be found using the following relation:

$$a_{total} = \frac{a_{wire} N}{f} \quad (5)$$

where  $a_{total}$  = cross-sectional area of NbTi wire  
=  $3.972 \times 10^{-7}$  m  
 $f$  = packing factor for hcp bundle  
= 0.74

The total cross-sectional radius may then be found as follows:

$$r = \sqrt{\frac{a_{total}}{\pi}} \quad (6)$$

For the purposes of this feasibility study, the design parameters have been set as follows. The enclosed area of the coil is  $1.829 \text{ m}^2$  yielding a circumference of 6.6 meters. It is desired to fully protect 1.5 meters, and thus the appropriate Störmer radius of 3.75 meters is specified. The weight to length ratio of the dewar is 10.51 kg/m, providing a total cryostat mass of 70 kg necessary for enclosing the coil. It is thus possible to determine the achievable protection level as a function of cryostat and coil total mass. The linear relationship found between the level of protection afforded and the cryostat/coil mass suggests that the final design of the experiment requires knowledge of the mass of all other components required for the mission.

### Coil Charging

Charging of the superconducting coil will be required to occur prior to experiment launch. Coils of this nature are routinely charged in nuclear magnetic resonance devices, and thus no novel technologies are necessary for this task. Three components are essentially needed: a superconducting switch, a cryostat interface, and a power supply. Basically, the superconducting switch consists of a portion of the superconducting wire which is thermally isolated from the rest of the coil. This portion is connected in parallel and leads to a junction board inside the cryostat. By activating a heater, a resistance is created in parallel with the main coil. By introducing main current leads across this resistance, the current in the coil can then be ramped up to the desired level. When that current level is reached, the heater is switched off and the current flows unimpeded as the previously heated section of the coil returns to a superconducting state. Additionally, dump resistors may be connected in parallel with the coil, allowing for a more controlled quench and thus absorbing power when the superconducting wire goes normal.

When the heater switch is closed, the resistive heater produces power according to the equation

$$P = I^2 R \tag{7}$$

Given a current in the heater of 60 mA and a resistance of 100 ohms, the power would be 0.36 W. With the switch in the open setting (heater on), a small resistance of approximately 10 ohms is created in parallel with the coil. It is then possible to begin introducing current into the coil.

Field instability is an issue that still must be considered in experimental design. The magnetic field induced by the coil will not stay at a constant level, and this problem is not easily rectified within the volume and weight restrictions of the payload. In principle, as the amount of current in each turn of the wire is increased, the tendency of the magnetic field to become unstable increases. In industry, these instabilities are managed by employing shim coils, which are smaller superconducting coils placed orthogonally to the main coil.<sup>10</sup> While effective, these shim coils require sizable control electronics assemblies, and thus appear impractical for use in this experimental design.

Charging the coil can only be accomplished if the coil is accessible through the cryostat. Simply, an extended and capped bore protruding from the cryostat would provide a buffer zone between the room temperature probe and the coil. The charging procedure would require that the cap be removed from the bore, and the charging lead inserted quickly to avoid loss of significant amounts of liquid helium. The lead is inserted halfway into the bore and allowed to cool for a short period of time. It is then fully inserted and plugged into the receptor socket, which connects to the junction board where the coil terminals are located.<sup>11</sup> One potential design could make use of an actively cooled baffle for the charging bore. This device utilizes an actively cooled heat sink to transfer heat away from the coil and inner cryostat to helium vapor which is vented to the environment.<sup>12</sup>

The power supply required for the charging will not affect the size or weight of the experimental payload, since charging will occur prior to launch. The required amperage is 320 A.

## Instruments

Three primary types of instruments are required for the experiment: radiation detectors, a gaussmeter (magnetometer), and a voltmeter. Additionally, temperature data will be required and thus thermocouples will be employed.

Radiation detection presents a design challenge, both in the choice of instruments and instrument layout within the experimental design. The use of a dosimeter was first considered, and space-proven instruments have already been demonstrated by several companies in this area. Dosimeters measure accumulated radiation dose, through the use of solid state detectors. A standard space-proven dosimeter can provide the following data: electron dose, electron flux, proton dose, proton flux, and nuclear star flux. The dosimeter has a field of view of  $2\pi$  steradians. However, the instantaneous radiation flux is most important experimentally. Therefore, alternatively, radiation detectors with the ability to measure both the accumulation and rate of radiation dose can be employed. At least three detectors would be required, with at least one mounted outside the magnetically protected region. Space-proven energetic particle detectors are also available, but may add unnecessary complexity to the data collection. Such instruments typically consist of a special telescope for sensing low energy protons and alphas, a dome-shaped detector for sensing medium energy protons and alphas in addition to electrons above 2 MeV, and a high-energy proton-alpha detector. These sensors are tied together with a signal analyzer unit/data processing unit which manages the various sensor outputs and routes them to telemetry devices.

A magnetometer is required for measuring the direction and magnitude of the magnetic field created by the superconducting coil. Once the coil goes normal, the magnetometer will measure the magnitude of the Earth's paleomagnetic field. The main function of the magnetometer is to quantify the size of the field produced and confirm that the coil is operational as designed. For low-earth orbital missions, fluxgate magnetometers with field ranges of  $\pm 55,000$  nT have been employed. Satellites placed in synchronous orbits have included magnetometers with field ranges of  $\pm 1,00$  nT, since the total field is much lower in this type of orbit. The final design characteristics of this instrument have not been established.

Finally, a voltmeter is required for measuring the voltage potential across the leads of the coil once the coil goes normal. A standard voltmeter with a 700 VAC range with a resolution of 0.1 V is acceptable.

## Telemetry

The onboard telemetry package should be capable of handling 112 KB/s with a self-contained power supply. A single-channel transponder is needed to relay data collected on radiation dosage, thermocouple readings, magnetometer output, and coil orientation. It is expected

that an S-band transponder will be used, with a downlink operating frequency of 2200 to 2300 MHz. A minimum of 5 watts is required for the transmission RF output.

### Power

Lithium thionyl chloride batteries have been chosen, which have a power density of approximately 150 watt•hours/kg. A major advantage of these batteries is that a weight savings of over 40% over commonly used silver-zinc batteries is realized, with similar performance characteristics. Typical power-to-weight ratios for various batteries are as follows: 350 W•hr/kg for lithium thionyl chloride, 140 W•hr/kg for silver-zinc, and 120 W•hr/kg for nickel metal hydride. This battery is space-qualified, with the ability to withstand the shock and vibrational stressing of launch. The battery has an operating temperature range of -55°C to 85°C.<sup>13</sup> Based on projected experimental requirements, it is expected that the battery will have a mass of no more than 20 kg, with a design life of 50 hours.

### Predicting Orbital Effects of the Ship's Field

The superconducting coil will interact with the earth's paleomagnetic field. If the interaction could be controlled, magnetic lift could potentially be created such that orbital maneuvering could be accomplished without fuel-based, energy and mass intensive thrusters. In the case of this coil, however, it should be noted that the coil will always align itself such that its dipoles will be oriented parallel to the local magnetic field. This, in effect, is a magnetic torque which forces a predictable alignment. The earth's magnetic field, approximately 0.5 Gauss, will impart a force of attraction on the coil in the radial direction, with the net effect being orbital decay rather than lift.

The magnitude of this magnetic force of attraction can be expressed in terms of the earth's polar angle, the magnetic moment of the coil, and the distance from the center of attraction.<sup>14</sup> This equation is as follows:

$$F_R = -1.46 \times 10^{-11} (IA) \left(\frac{r_0}{r}\right)^4 [R(\theta)r + T(\theta)\theta] \quad (8)$$

where I = current in Amp•turns  
 A = area enclosed by coil  
 $\theta$  = polar angle  
 $r_0/r$  = altitude of coil, expressed in earth radii

The functions  $R(\theta)$  and  $T(\theta)$  are magnetic propulsion functions as follows:

$$R(\theta) = (3 \cos^2 \theta + 1)^{0.5} \quad (9)$$

$$T(\theta) = (\frac{1}{2})(\sin 2\theta)(3 \cos^2 \theta + 1)^{0.5}$$

By averaging the magnetic propulsion functions over a full orbit (i.e..  $\Delta\theta=2\pi$  rads), it is found that the average radial force component is on the order of  $F_R=9.64 \times 10^{-6}\text{N}$ . This translates into a maximum force of approximately  $1.29 \times 10^{-6}\text{N}$  (at  $\theta=2\pi$  rads) and a minimal force of  $0.646 \times 10^{-6}\text{N}$  (at  $\theta=\pi/2$  rads). The net effect of this radial force of attraction will translate into a loss of kinetic energy and the ship will be unable to sustain a constant altitude during orbit. The magnitude of this orbital decay was calculated in the following fashion.

Elementary physics relates the tangential velocity of the ship to the altitude of orbit and the eccentricity of the path taken.<sup>15</sup> The equation relating these variables is as follows:

$$V_T^2 = 2gR^2[(1/r) - (1/2a)] \quad (10)$$

where  $a$  = perigee altitude

To simplify calculations, a circular orbit (i.e.. eccentricity=0) is assumed such that  $a=r=100 \text{ km} + R_{\text{earth}}$ . On this basis, it is found that the tangential velocity of the coil is approximately 7.844 km/s. This translates into a period given by the following equation:

$$\tau = \frac{2\pi a^{3/2}}{R\sqrt{g}} \quad (11)$$

The period is found to be 1.441 hours, or approximately 16.65 orbits/day. Given that the change in total energy is equal to the change in kinetic energy of the coil, it is found that the coil will undergo a small orbital decay due to this magnetic force of attraction, on the order of 8.64 m/day.

### Scientific Experiment

A magnetic field can be used to generate a voltage by two primary methods, with said voltage being termed either induced emf or motional emf. Induced emf is generally associated with the rectangular loops used in motors and generators.

At the time that the superconducting coil goes normal (i.e.,  $t=96$  h), the coil will still be passing through the earth's magnetosphere. Consequently, there will be an induced emf created due to the interaction with the earth's magnetic field. As the ship cuts the magnetic field lines of the earth, the induced emf will be created as predicted by Faraday's law. This is given as follows:

$$-\frac{d\phi}{dt} = \varepsilon \quad (12)$$

where  $\phi$  = the magnetic flux  
 =  $NBA\cos\theta$

One problem that arises is that the opposing sides of the coil effectively cancel each other out. For this reason, it is necessary to partially shield the coil in order to induce a significant emf, on the order of 100 V. Assuming that this is feasible, the power dissipated through such a process is as follows:

$$P = i^2 R \quad (13)$$

where  $i$  = the induced current  
 =  $V/R$   
 $R$  = the resistance of the non-superconducting NbTi wire

The coil resistance is calculated as follows:

$$R = \frac{\rho L}{A} \quad (14)$$

where  $\rho$  = the resistivity of NbTi  
 =  $1.39 \times 10^{-8} \Omega \cdot m$   
 $L$  = total length of coil (m)  
 =  $5.75 \times 10^3$  km  
 $A$  = cross-sectional area of the coil ( $d=10$  mil)  
 =  $50.7 \times 10^{-9} m^2$

The resistance is therefore approximately 1573.2  $\Omega$ . Given that the target value for the induced emf is approximately 100 volts, the current is found to be 63.5 mA. Consequently, the power

dissipated in the coil is approximately 6.36 watts. The total energy dissipation can be found as follows:

$$\Delta E = P \Delta t \tag{15}$$

Over the course of two weeks (after the coil goes normal), this will be approximately  $7.6 \times 10^6$  joules. Relative to the kinetic energy of the ship at a 100 km orbit ( $\sim 3.03 \times 10^{10}$  J), this change in energy is negligible and will not affect the orbital decay rate significantly.

### Coil Orientation

During orbit, the coil and its associated magnetic dipole will be constantly interacting with the natural paleomagnetic field of the earth. Without the aid of torquer bars, an intricate arrangement of three independent gyroscopes, or some other orientation devices, the coil will undergo changes in orientation due to the interaction between the two magnetic fields. Thus, there is a torque imposed on the coil by this magnetic interaction which always tends to orient the dipole parallel to the local field. The most stable position tends to be one of polar attraction in which the induced south pole of the coil is oriented towards the north pole of the earth.

As the coil orbits the earth, there will be a magnetic torque imposed on the coil which will advantageously orient the coil with respect to the earth's paleomagnetic field. This torque is expressed as follows:

$$\mathbf{T} = \mathbf{M} \times \mathbf{B} \tag{16}$$

where  $\mathbf{T}$  = the magnetic torque acting on the coil (N·m)  
 $\mathbf{M}$  = the coil magnetic dipole moment (A·m<sup>2</sup>)  
 $\mathbf{B}$  = the magnetic field (webers/m<sup>2</sup>)

In the specific case of the coil studied herein, the magnetic dipole moment is  $4.767 \times 10^5$  ampere-turns·m<sup>2</sup>, and the magnetic field of the earth is approximately 0.5 Gauss ( $5 \times 10^{-5}$  T). It should be noted that the magnetic torque acting on the coil will be a vector quantity. However, the maximum torque will occur when the dipoles of the coil and the earth's magnetic poles are orthogonal (i.e., the axis of each loop is perpendicular to the magnetic field). In this case, the maximum torque can be expressed as the scalar product of the magnetic dipole moment and the magnetic field. The maximum torque is found to be 23.835 Newton·m.

The magnetic torque will impose an angular acceleration on the coil, given as follows:

$$\alpha = \frac{T}{I} \tag{17}$$

where  $\alpha$  = the angular acceleration  
 $T$  = the magnetic torque  
 $I$  = the mass moment of inertia  
 $\sim 80 \text{ kg}\cdot\text{m}^2$

Thus, the coil would be expected to undergo an angular acceleration of  $2.98 \times 10^{-1} \text{ rads/s}^2$ . The coil alignment time can then be found as follows:

$$\Delta\theta = \omega t + (1/2)\alpha t^2 \tag{18}$$

The coil will theoretically align itself in 3.25 seconds, assuming no oscillatory behavior.

Although this is a simplified approach to determining the orbital kinetics, it provides an order of magnitude approximation of the angular forces imparted on the coil. More realistically, the angular acceleration will be a function of orientation and the value calculated is the maximum value. As the coil's angle of orientation slowly changes from  $\pi/2$  to 0 radians, the angular acceleration of the coil will decrease. However, the angular velocity  $\omega$  continues to increase until the coil reaches an orientation such that the dipole moment of the coil is aligned with the earth's paleomagnetic field. At this point, the angular velocity will begin to decrease, with the net effect being a small oscillation about the stable axis due to the magnetic torque. Therefore, the actual stabilization time will be somewhat longer than estimated.

### Mass Shielding for the Payload

Several areas of the experimental payload will require mass shielding. One example of this is that the radiation detectors will need to be shielded from the radiation incident from other areas of the payload beside that penetrating the magnetic shielding barrier alone. Directional, mass shielding must be employed. One possible approach to this problem would be to stop the incoming flux of electrons using a lead barrier. Lead is a practical shielding material due to its high mass absorption coefficient, which varies as a function of wavelength. The ability of lead to stop penetration of high energy particles is represented as follows:<sup>16</sup>

$$I = I_0 e^{-\left(\frac{\mu}{\rho}\right)\rho x} \quad (19)$$

where  $I/I_0$  = the proportion of high energy particles stopped  
 $\mu$  = mass absorption coefficient  
 $\sim 100 \text{ cm}^{-1}$   
 $\rho$  = density of lead  
 $\sim 11.34 \text{ g/cm}^3$   
 $x$  = thickness of lead barrier (cm)

It is also true that the wavelength of the incoming radiation is inversely proportional to the particle's maximum cut-off energy such that:<sup>17</sup>

$$\lambda[\text{\AA}] = \frac{12.4}{KE[\text{KeV}]} \quad (20)$$

Assuming that the incoming radiation will have a maximum cut-off energy on the order of 1 MeV, this radiation will have a wavelength of 0.0124 Å. The mass absorption coefficient for lead is tabulated as a function of this wavelength in Table 1. Using a linear regression analysis, a function relating the mass absorption coefficient to the wavelength has been determined:

$$\left(\frac{\mu}{\rho}\right) = 28.23\lambda^3 + 122.24\lambda^2 - 266.40\lambda + 257.9 \quad (21)$$

where  $\lambda$  = wavelength (Å)

Table 1 Mass Absorption  
Coefficient for Lead

$\lambda$ (Å)	$\mu/\lambda$ (cm <sup>2</sup> /s)
0.7	141
1.4	202
1.7	297
2.1	499

Though this mathematical model works well for relatively large wavelengths radiation (i.e., low energy), it predicts large mass absorption coefficients at small wavelengths ( $\lambda < 1\text{\AA}$ ). The actual plot of mass absorption coefficient as a function of wavelength includes a number of inflection points. In fact, the mass absorption function undergoes a number of significant jumps at these "absorption edges" denoted by the subscripts K, L, and M. The wavelength of the radiation for which the shield is designed, approximately  $0.01\text{\AA}$ , places it just below the K absorption edge (which occurs at approximately  $0.05\text{\AA}$  for lead). A logarithmic approximation can thus be used to predict the mass absorption in this range. By studying the transition at the K absorption edge of other metals, it is found that the slope of the mass absorption coefficient as a function of wavelength plot is approximately  $0.125 \times 10^{-12}\text{ cm}^2/\text{g}\cdot\text{nm}$ . Thus, it is found that the mass absorption coefficient at  $0.01\text{\AA}$  is approximately  $0.236\text{ cm}^2/\text{g}$ . It is finally found that the minimum lead thickness for shielding the payload from 99% of the incoming radiation ( $\beta$  particles) is approximately 1.7 cm. Thus, only select regions can be fully mass-shielded.

## Conclusion

An experimental magnetic shielding payload launched into polar orbit is feasible within the design size and weight constraints. This payload can be design, constructed, and tested at remarkably low cost using many of the technologies developed for lightsats. The scientific experiments offer interdisciplinary research involving the atmospheric and high-energy physics communities, the aerospace community, and the engineering community with the potential for major contributions to our understanding of active radiation shielding techniques, microcirculation in the auroral zones of the atmosphere, as well as other electrical and physical phenomena involving large magnetic fields.

---

<sup>1</sup> Adolph S. Jursa, Ed., Handbook of Geophysics and the Space Environment, United States Air Force (Virginia, 1985), 1, 18-19.

<sup>2</sup> Peter Berlin, The Geostationary Applications Satellite, Cambridge University Press (New York, 1988), 71.

<sup>3</sup> Ibid, 3.

<sup>4</sup> A.L. Vampola, "Radiation Effects on Space Systems and Their Modeling", Space Systems and Their Interactions with Earth's Space Environment, Eds. Henry B. Garrett and Charles P. Pike, American Institute of Aeronautics and Astronautics (New York, 1980), 240.

<sup>5</sup> Jursa, 3-6.

<sup>6</sup> Vampola, 341.

<sup>7</sup> Ibid.

- 
- <sup>8</sup>R.A. English, R.E. Benson, J.V. Basley and C.M. Barnes, Apollo Experience Report - Protection Against Radiation, NASA, Washington, D.C. NASA TN D-7080, 2, 1973.
- <sup>9</sup>Gordon R. Woodcock, Space Stations and Platforms, Orbit Book Company (Malabar, Florida, 1986), 64.
- <sup>10</sup>Superconducting Magnet System, Oxford Instruments Ltd., manual.
- <sup>11</sup> Ibid.
- <sup>12</sup> William C. Chen and Daniel C. Woods, Actively Cooled Baffle for Superconducting Magnet Penetration Wall, U.S. Patent No. 5,265,430, November 30, 1993.
- <sup>13</sup> Pinakin M. Shah, "A high power lithium thionyl chloride battery for space applications", *Journal of Power Sources*, 43-44 (1993) 317-326.
- <sup>14</sup> Robert M. Zubrin, "The Use of Magnetic Sails to Escape from Low Earth Orbit", *Journal of the British Interplanetary Society*, Vol. 46 (1993), pp. 3-10.
- <sup>15</sup> J. L. Meriam and L. Kraige, Engineering Mechanics: Dynamics, John Wiley & Sons, Inc., New York, NY, 1992, pp. 230-236.
- <sup>16</sup> B. D. Cullity, Elements of X-ray Diffraction, 2nd Ed., Addison-Wesley Publishing Company, Inc. (Reading, MA, 1978) p. 13.
- <sup>17</sup> Ibid., 18.

Figure 3 The senior mechanical engineering design class met with David Sollberger of NASA Kennedy Space Center to discuss spacecraft design parameters and strategies.



**Appendix A**  
**Payload Diagrams**

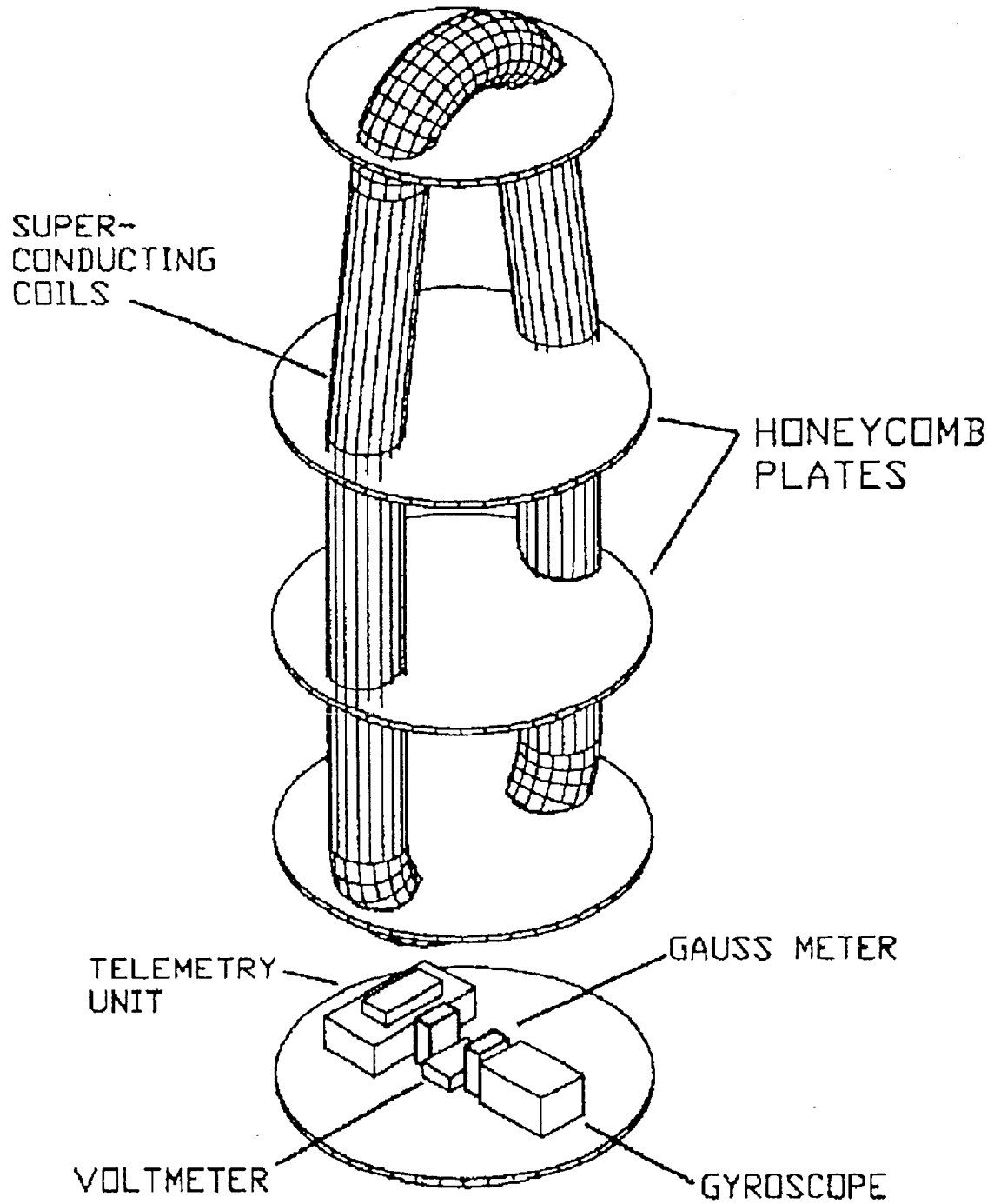


Figure 4 Payload configuration showing superconducting coil with cryostat, plates, and instruments

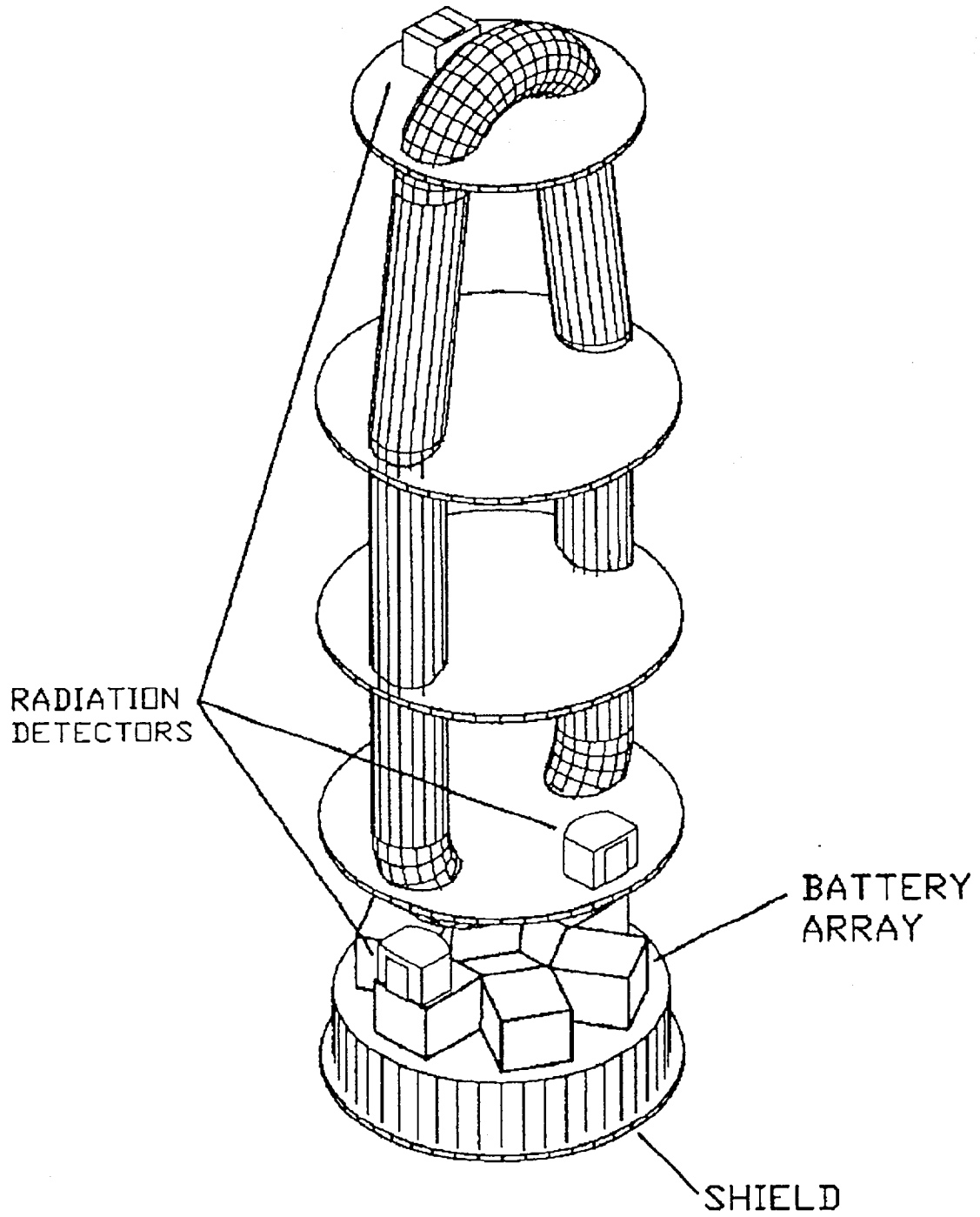


Figure 5 Payload configuration showing shield, battery array,  
and radiation detectors

HARD MOUNTING ATTACH POINTS

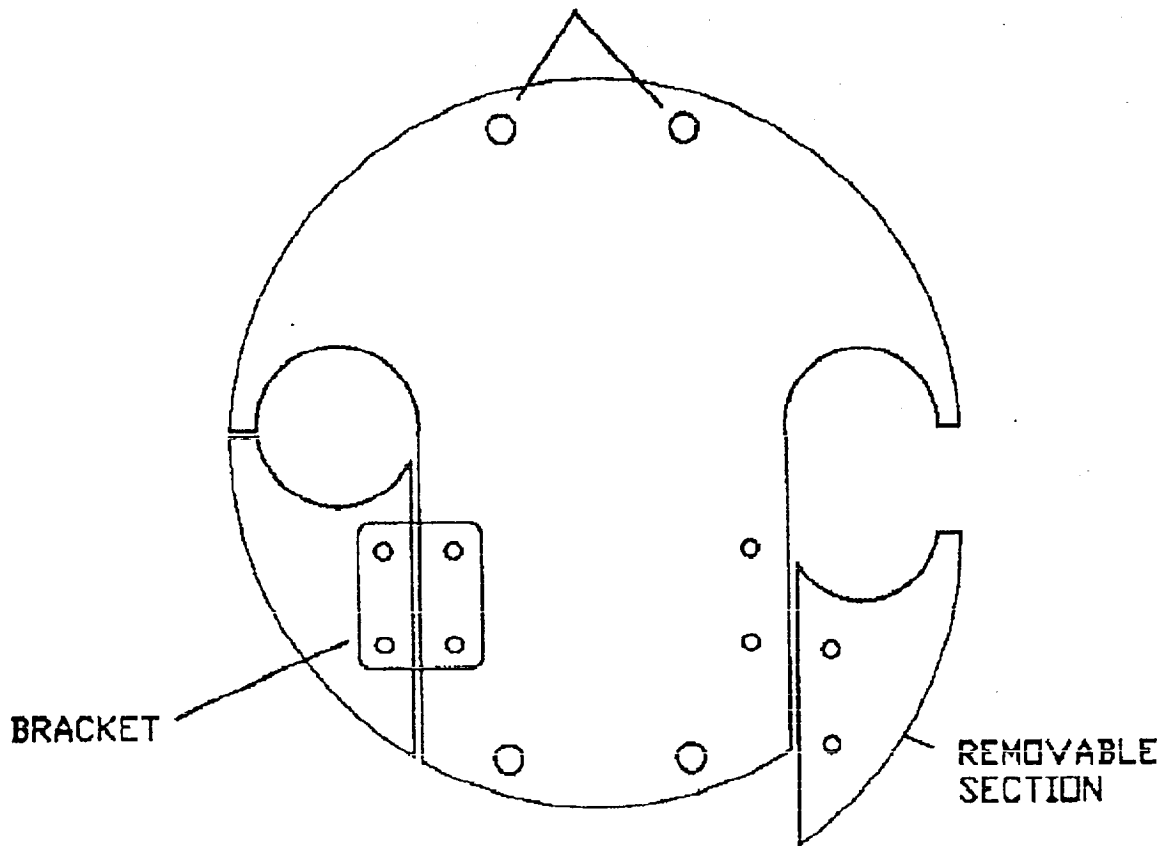


Figure 6 Removable mounting plate sections allow for ease of cryostat installation

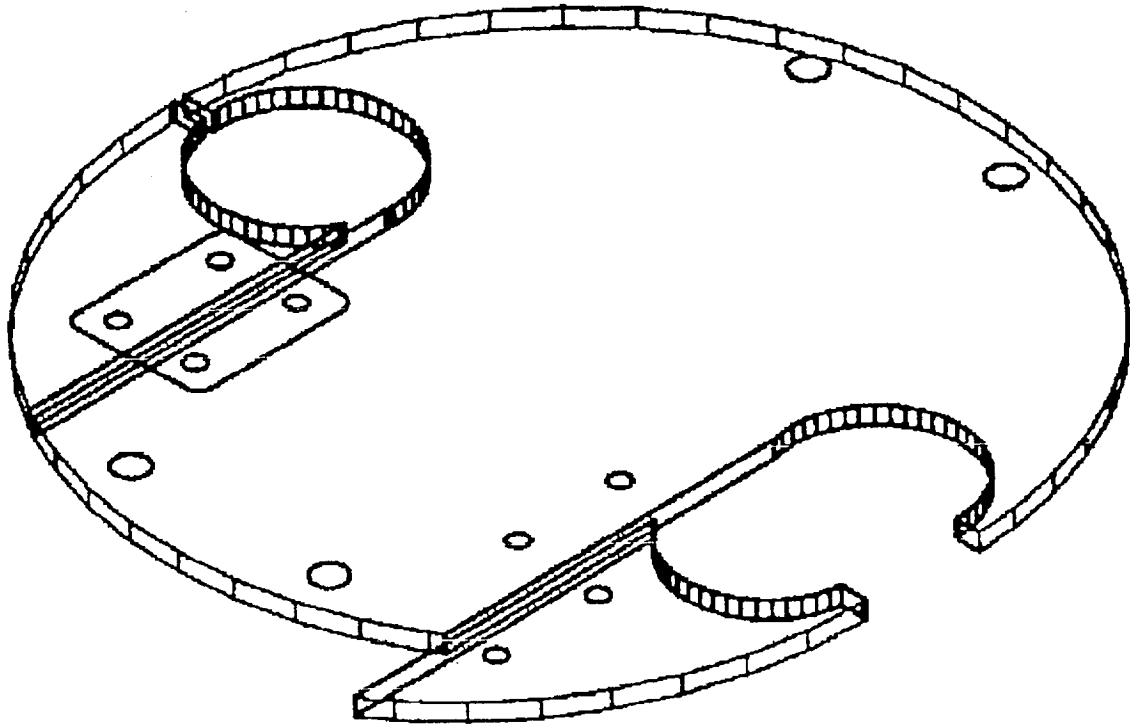


Figure 7 Mounting plate details